Metal-Assisted Cleavage of the Porphyrinogen Skeleton: Reaction of *meso*-Octaethylporphyrinogen Complexes with Benzaldehyde

Giovanna Solari,[†] Euro Solari,[†] Gilles Lemercier,[†] Carlo Floriani,*[,†] Angiola Chiesi-Villa,[‡] and Corrado Rizzoli[‡]

Institut de Chimie Minérale et Analytique, Université de Lausanne, BCH, CH-1015, Lausanne, Switzerland, and Dipartimento di Chimica, Università di Parma, I-43100 Parma, Italy

Received December 4, 1996

Introduction

A major perspective in metal-assisted processes is the modification and reactivity of large and relevant structures. Our target molecule in the present study is the porphyrinogen skeleton, which is the chemical and biochemical precursor of porphyrins.[1] Its complexation to metals and the consequent chemistry were unsuccessful because of its oxidative instability and fast conversion to porphyrins.[1] The metal−porphyrinogen chemistry has been only recently developed using the *meso*-octaalkylporphyrinogen,[2] the fully alkylated form of the usual *meso*-tetrahydrotetraalkylporphyrinogen. The metal-bonded *meso*-octaalkylporphyrinogen[3−7] was investigated from the point of view of a precursor of "artificial porphyrins"[3,4] and as a very versatile bifunctional ligand in organometallic reactions, when assisting the C−H bond activation[5] and the homologation of the pyrrole to the pyridine ring.[6] In the latter reaction pyrrole is attacked by an electrophilic carbenium ion.[7] We report here the metal-assisted reactions of benzaldehyde on titanium− and zirconium−*meso*-octaethylporphyrinogen which lead to the modification and cleavage of the tetrapyrrolic structure as a function of the oxophilicity of the metal.

Experimental Section

General Procedure. All reactions were carried out under an atmosphere of purified nitrogen. Solvents were dried and distilled before use by standard methods. The syntheses of **1**[8] and **2**[9] were performed as reported. NMR spectra were measured on 200-AC and 400-DPX Bruker instruments.

Preparation of 3. A toluene (80 mL) solution of freshly distilled benzaldehyde (1 mL, 9.7 mmol) was added under nitrogen to a dark-green solution of **1** (4.75 g, 6.5 mmol) in toluene (300 mL) at −30 °C. When the temperature was allowed to reach room temperature, the solution turned red. After 48 h of stirring, the mixture was evaporated to dryness. *n*-Hexane (150 mL) was added, and an ocre-red powder was obtained (3.9 g, 85%). Anal. Calcd for $C_{43}H_{54}N_4OTi$: C, 74.80; H, 7.90; N, 8.10. Found: C, 74.20; H, 7.90; N, 7.80. ^{1}H NMR (C_6D_6, 200 MHz, room temperature): δ 6.94−6.80 (m, 5H, ArH), 6.78 (d, 1H, J = 5.3 Hz, C_4H_2N), 6.69 (s, 2H, C_4H_2N), 6.32 (d, 1H, J = 3.4 Hz, C_4H_2N), 6.27 (d, 1H, J = 3.4 Hz, C_4H_2N), 6.06 (d, 1H, J = 3.4 Hz, C_4H_2N), 6.03 (d, 1H, J = 3.4 Hz, C_4H_2N), 5.88 (s, 1H, PhC*H*O), 5.65 (d, 1H, J = 5.3 Hz, C_4H_2N), 2.77 (m, 1H, CH_2), 2.22 (m, 8H, CH_2), 1.92 (m, 4H, CH_2), 1.59 (m, 3H, CH_2), 1.03 (t, 3H, J = 7.3 Hz, CH_3), 0.9 (t, 3H, J = 7.3 Hz, CH_3) overlapping with 0.89 (t, 3H, J = 7.3 Hz, CH_3), 0.83 (t, 3H, J = 7.3 Hz, CH_3) overlapping with 0.82 (t, 3H, J = 7.3 Hz, CH_3), 0,72 (t, 3H, J = 7.3 Hz, CH_3), 0.64 (t, 3H, J = 7.3 Hz, CH_3), 0.52 (t, 3H, J = 7.3 Hz, CH_3). Red crystals suitable for X-ray analysis were obtained from a saturated benzene solution (1.3 g in 60 mL) upon addition of hexane (100 mL). Compound **3** forms independently of the Ti/PhCHO molar ratio.

Hydrolysis of 3. A toluene (40 mL) solution of **3** (0.64 g, 0.75 mmol) was hydrolyzed with degassed water. The mixture turned orange-yellow and was stirred for 1 night under nitrogen. Extraction with toluene and evaporation to dryness gave pure *meso*-octaethylporphyrinogen (0.38 g, 75%).

Reactivity of 3 with LiMe. LiMe (1.3 mL, 1.56 M, 2.1 mmol) was slowly added to a toluene (150 mL) solution of **3** (1.4 g, 2.0 mmol) at −50 °C. Warming to room temperature resulted in the solution turning gray-green (complex **1**). After being stirred for 3 days, the solution turned blue-green and was then evaporated to dryness and hydrolyzed to give *meso*-octaethylporphyrinogen.

Preparation of 6. Freshly distilled PhCHO (1.24 g, 11.7 mmol) was added dropwise to a yellow toluene (100 mL) solution of **2** (4.09 g, 5.85 mmol) and the resulting deep red solution was stirred at room temperature for 5 h. The solution was evaporated to dryness and the residue triturated with *n*-hexane (80 mL) to give an orange-yellow powder which was collected and dried *in vacuo* (1.5 g, 30%). Crystals suitable for X-ray analysis were grown in *n*-hexane. Anal. Calcd for

* To whom correspondence should be addressed.
† University of Lausanne.
‡ University of Parma.

(1) (a) *Porphyrins and Metalloporphyrins*; Smith, K. M., Ed.; Elsevier: Amsterdam, The Netherlands, 1975 *The Porphyrins*; Dolphin, D, Ed.; Academic: New York, 1978. (b) Mashiko, T; Dolphin, D. In *Comprehensive Coordination Chemistry*; Wilkinson, G., Gillard, R. D., McCleverty, J. A., Eds.; Pergamon: Oxford, U.K., 1987; Vol. 2, Chapter 21.1, p 855. (c) Kim, J. B.; Adler, A. D.; Longo, R. F. In *The Porphyrins*; Dolphin, D., Ed.; Academic: New York, 1978; Vol. 1, Part A, p 85. Mauzerall, D. *Ibid.*, Vol. 2, p 91. (d) Lindsey, J. S.; Schreiman, I. C.; Hsu, H. C.; Kearney P. C.; Marguerettaz, A. M. *J. Org. Chem.* **1987**, *52*, 827. Lindsey, J. S.; Wagner, R. W. *J. Org. Chem.* **1989**, *54*, 828. (e) *Biosynthesis of Tetrapyrroles*, Jordan, P. M., Ed.; Elsevier: New York, 1991.

(2) (a) Baeyer, A. *Chem. Ber.* **1886**, *19*, 2184. (b) Fischer, H.; Orth, H. *The Chemistry of Pyrroles;* Akademische Verlagsgesellschaft: Leipzig, Germany, 1934; p 20. (c) Dennstedt, M.; Zimmermann, J. *Chem. Ber.* **1887**, *20*, 850 and 2449; **1888**, *21*, 1478. (d) Dennstedt, D. *Chem. Ber.* **1890**, *23*, 1370. (e) Chelintzev, V. V.; Tronov, B. V. *J. Russ. Phys. Chem. Soc.* **1916**, *48*, 105, 127. (f) Sabalitschka, Th.; Haase, H. *Arch. Pharm.* **1928**, *226*, 484. (g) Rothemund, P.; Gage, P. L. *J. Am. Chem. Soc.* **1955**, *77*, 3340.

(3) Floriani, C. *Pure Appl. Chem.* **1996**, *68*, 1 and references therein.

(4) (a) Jubb, J.; Floriani, C.; Chiesi-Villa, A.; Rizzoli, C. *J. Am. Chem. Soc.* **1992**, *114*, 6571. (b) Piarulli, U.; Floriani, C.; Chiesi-Villa, A.; Rizzoli, C. *J. Chem. Soc., Chem. Commun.* **1994**, 895. (c) De Angelis, S.; Solari, E.; Floriani, C.; Chiesi-Villa, A.; Rizzoli, C. *J. Am. Chem. Soc.* **1994**, *116*, 5691. (d) De Angelis, S.; Solari, E.; Floriani, C.; Chiesi-Villa, A.; Rizzoli, C. *J. Am. Chem. Soc.* **1994**, *116*, 5702. (e) Floriani, C. *Transition Metals in Supramolecular Chemistry*; Fabbrizzi, L., Poggi, A., Eds; Nato ASI Series; Kluwer: Dordrecht, The Netherlands, 1994; Vol. 448, pp *448*, 191−209. (f) Piarulli, U.; Solari, E.; Floriani, C.; Chiesi-Villa, A.; Rizzoli, C. *J. Am. Chem. Soc.* **1996**, *118*, 3634−3642.

(5) (a) Jacoby, D.; Isoz, S.; Floriani, C.; Chiesi-Villa, A.; Rizzoli, C. *J. Am. Chem. Soc.* **1995**, *117*, 2805. (b) Isoz, S.; Floriani, C.; Schenk, K.; Chiesi-Villa, A.; Rizzoli, C. *Organometallics* **1996**, *15*, 337.

(6) Jacoby, D.; Floriani, C.; Chiesi-Villa, A.; Rizzoli, C. *J. Am. Chem. Soc.* **1993**, *115*, 7025. Jacoby, D.; Isoz, S.; Floriani, C.; Chiesi-Villa, A.; Rizzoli, C. *J. Am. Chem. Soc.* **1995**, *117*, 2793. Floriani, C. In *Stereoselective Reactions of Metal-Activated Molecules*; Werner, H., Sundermeyer, J., Eds.; Vieweg: Wiesbaden, Germany, 1995; p 97. Jacoby, D.; Isoz, S.; Floriani, C.; Schenk, K.; Chiesi-Villa, A.; Rizzoli, C. *Organometallics* **1995**, *14*, 4816.

(7) Tatsumi, K.; Nakamura, A.; Hofmann, P.; Stauffert, P.; Hoffmann, R. *J. Am. Chem. Soc.* **1985**, *107*, 4440. Martin, B. D.; Matchett, S. A.; Norton, J. R.; Anderson, O. P. *J. Am. Chem. Soc.* **1985**, *107*, 7952. Roddick, D. M.; Bercaw, J. E. *Chem. Ber.* **1989**, *122*, 1579. Hofmann, P.; Stauffert, P.; Frede, M.; Tatsumi, K. *Chem. Ber.* **1989**, *122*, 1559. Hofmann, P.; Stauffert, P.; Tatsumi, K.; Nakamura, A.; Hoffmann, R. *Organometallics* **1985**, *4*, 404. Tatsumi, K.; Nakamura, A.; Hofmann, P.; Hoffmann, R.; Moloy, K. G.; Marks, T. J. *J. Am. Chem. Soc.* **1986**, *108*, 4467.

(8) (a) De Angelis, S.; Solari, E.; Floriani, C.; Chiesi-Villa, A.; Rizzoli, C. *Angew. Chem., Int. Ed. Engl.* **1995**, *34*, 1092. (b) De Angelis, S.; Solari, E.; Floriani, C.; Chiesi-Villa, A.; Rizzoli, C. *Organometallics* **1995**, *14*, 4505.

(9) (a) Jacoby, D.; Floriani, C.; Chiesi-Villa, A.; Rizzoli, C. *J. Am. Chem. Soc.* **1993**, *115*, 3595. (b) Jacoby, D.; Floriani, C.; Chiesi-Villa, A.; Rizzoli, C. *J. Chem. Soc., Chem. Commun.* **1991**, 790.

S0020-1669(96)01446-2 CCC: $14.00

Table 1. Experimental Data for the X-ray Diffraction Studies on Crystalline Complexes **3, 6**, and **7**

	complex		
	3	**6**	**7**
formula	$C_{43}H_{54}N_4OTi$	$C_{50}H_{60}N_4O_2Zr$	$C_{82}H_{76}N_4O_8Zr_2$
a, Å	11.447(3)	18.552(3)	12.205(3)
b, Å	18.842(4)	25.784(4)	22.265(4)
c, Å	17.642(2)	17.561(3)	13.041(3)
α, γ, deg	90	90	90
β, deg	101.68(1)	90	105.15(2)
V, Å^3	3726.3(13)	8400(2)	3420.7(13)
Z	4	8	2
fw	690.8	840.3	1428.0
space group	$P2_1/n$ (No. 14)	*Pbca* (No. 61)	$P2_1/c$ (No. 14)
t, °C	−140	−140	−140
λ, Å	1.541 78	1.541 78	1.541 78
ρ_{calc}, g cm^{-3}	1.231	1.329	1.386
μ, cm^{-1}	22.23	24.96	30.04
transm coeff	0.809−1.000	0.720−1.000	0.708−1.000
R^a	0.044	0.045	0.049
w$R2^a$	0.123	0.124	0.142

[a] $R = \sum|\Delta F|/\sum|F_o|$ calculated on the unique observed data [$I > 2\sigma(I)$]. w$R2 = [\sum w|\Delta F^2|^2/\sum w|F_o^2|^2]^{1/2}$ calculated on the unique data having $I > 0$.

$C_{50}H_{66}N_4O_2Zr$: C, 70.96; H, 7.86; N, 6.62. Found: C, 70.99; H, 7.45; N, 6.67. ^{1}H NMR (C_6D_6, 200 MHz, 298 K): δ 7.62 (m, 2H, ArH), 7.10 (m, 10H, ArH) overlapping with 7.07 (d, 2H, C_4H_2N), 6.84 (m, 2H, C_4H_2N), 6.64 (d, $J = 4.88$ Hz, 1H, C_4H_2N), 6.32 (s, 2H, C_4H_2N), 6.22 (d, $J = 3.90$ Hz, 1H, C_4H_2N), 6.01 (d, $J = 4.88$ Hz, 2H), 4.95 (s, 2H, $PhCH_2O$), 3.03 (m, 1H, CH_2), 2.46 (m, 7H, CH_2), 2.10 (m, 4H, CH_2), 1.76 (m, 4H, CH_2), 1.37 (t, $J = 7.32$ Hz, 3H, CH_3), 1.21 (t, $J = 7.32$ Hz, 3H, CH_3), 1.05 (m, 6H, CH_3), 0.77 (t, $J = 7.32$ Hz, 3H, CH_3) overlapping with 0.67 (m, 9H, CH_3).

Preparation of 7. Freshly distilled PhCHO (5.25 g, 49.0 mmol) was added dropwise to a yellow toluene (100 mL) solution of **2** (4.22 g, 6.0 mmol), and the resulting deep red solution was stirred at room temperature for 5 h. The solvent was partially evaporated, and *n*-hexane (100 mL) was added. An orange-yellow powder formed and was then collected and dried *in vacuo* (3.4 g, 40%). Crystals suitable for X-ray analysis were grown in a mixture of toluene/Et_2O. Anal. Calcd for $C_{82}H_{76}N_4O_8Zr_2$: C, 68.97; H, 5.36; N, 3.92. Found: C, 69.25; H, 5.35; N, 3.77. ^{1}H NMR (C_6D_6, 200 MHz, 298 K): δ 7.79 (m, 8H, ArH), 7.27 (m, 10H, ArH), 7.12 (m, 10H, ArH), 6.93 (m, 8H, ArH), 6.75 (s, 8H, C_4H_2N), 6.34 (m, 4H, ArH), 5.85 (s, 4H, $PhCH_2O$), 4.42 (s, 4H, $PhCH_2O$), 1.82 (q, $J = 7.3$ Hz, 4H, CH_2), 1.76 (q, $J = 7.3$ Hz, 4H, CH_2), 0.61 (t, $J = 7.3$ Hz, 6H, CH_3), 0.36 (t, $J = 7.3$ Hz, 6H, CH_3). The best way to run the reaction is to use a 1:4 Zr/PhCHO ratio. Compound **7** can be equally well obtained reacting **6** with 2 equiv of PhCHO.

X-ray Crystallography for Complexes 3, 6, and 7. Intensity data were collected at low temperature on a single-crystal four-circle diffractometer. Crystal data and refinement details for complexes **3**, **6**, and **7** are given in Table 1. The reduced cells were obtained with use of TRACER.[10] For intensities and background individual reflection profiles were analyzed.[11] Intensity data were corrected for Lorentz and polarization effects and for absorption.[12] The function minimized during the full-matrix least-squares refinement was $\sum w|\Delta F^2|^2$ using a weighting scheme based on counting statistics.[13] Anomalous scattering corrections were included in all structure factor calculations.[14b] Scattering factors for neutral atoms were taken from ref 14a for non-hydrogen atoms and from ref 15 for H. Among the low-angle reflections, no correction for secondary extinction was deemed necessary.

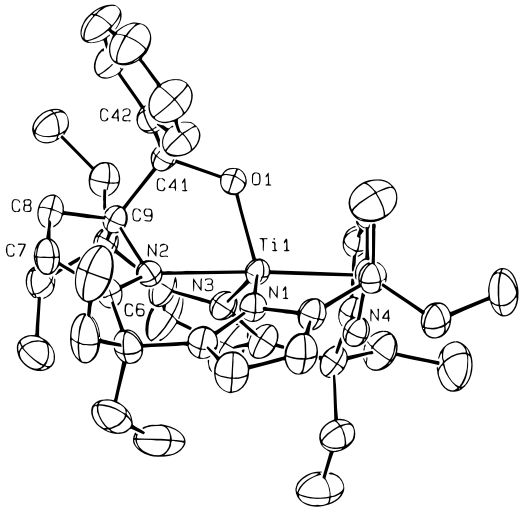

Figure 1. ORTEP view of the structure of complex **3** (50% probability ellipsoids).

The structures were solved by the heavy-atom method (Patterson and Fourier syntheses). Refinement was first done isotropically and then anisotropically for all the non-H atoms using the unique data with $I > 0$. In complex **7** the C62−C67 aromatic ring was found to be disordered over two positions called A and B which were isotropically refined with a site occupation factor of 0.5 by applying a rigid body constrain (D_{6h} symmetry). The H atoms except those associated with the disordered benzylic group, which were ignored, were located in ΔF maps and introduced in the refinements as fixed contributors with isotropic *U* values fixed at 0.05 Å^2 for all complexes. The final difference map showed no unusual features, with no significant peak above the general background. Selected bond distances and angles are given in Tables 2−4 for complexes **3**, **6**, and **7**, respectively.[16]

Results and Discussion

The reaction of **1**[8] and **2**[5,6,9] with PhCHO was carried out in toluene at room temperature, with various stoichiometric ratios depending on the metal. In the case of **1**, regardless of the stoichiometric ratio, reaction conditions, and time, we obtained **3** exclusively and almost quantitatively. The genesis of **3** can be easily understood by assuming precoordination of benzaldehyde to titanium, which would enhance its electrophilicity, followed by the attack of benzaldehyde on the α-pyrrole carbon of one of the pyrrolyl anions of the macrocycle. The coordination of benzaldehyde to the metal center is a general event in such reaction (*vide infra* the reactivity of zirconium). In the case of titanium we did not observe any further reaction with PhCHO, as expected due to the lower Lewis acidity of the metal on **3** *vs* **1**. The addition of PhCHO to **1** gave rise to a novel pentadentate tetraanionic N_4O macrocyclic ligand. The reaction of **1** with PhCHO introduced two chiral centers, though a single diastereoisomer has been observed in the case of **3**. The steric hindrance of the *meso*-carbon and the phenyl group prevents, very probably, the formation of the other diastereoisomer. The red crystals of **3** have been characterized, including an X-ray analysis. The structure of **3** is reported in Figure 1, with structural parameters in Table 2.

The pyrrole rings containing the N1, N2, N3, and N4 nitrogen atoms are referred as A, B, C, and D, respectively. The increased electron demand by titanium in **3** along with the steric

(10) Lawton, S. L.; Jacobson, R. A. TRACER, A Cell Reduction Program; Ames Laboratory, Iowa State University of Science and Technology: Ames, IA, 1965.
(11) Lehmann, M. S.; Larsen, F. K. *Acta Crystallogr., Sect. A: Cryst. Phys., Diffr., Theor. Gen. Crystallogr.* **1974**, *A30*, 580.
(12) North, A. C. T.; Phillips, D. C.; Mathews, F. S. *Acta Crystallogr., Sect. A: Cryst. Phys., Diffr., Theor. Gen. Crystallogr.* **1968**, *A24*, 351.
(13) Sheldrick, G. M. *SHELX*92 *Gamma Test*: *Program for Crystal Structure Refinement*; University of Göttingen: Göttingen, Germany, 1992.
(14) *International Tables for X-ray Crystallography*; Kynoch Press: Birmingham, England, 1974; Vol IV: (a) p 99; (b) p 149.
(15) Stewart, R. F.; Davidson, E. R.; Simpson, W. T. *J. Chem. Phys.* **1965**, *42*, 3175.
(16) See paragraph at the end of paper regarding Supporting Information.

Table 2. Selected Interatomic Distances (Å) and Angles (deg) for Complex **3**

Ti1−O1	1.850(2)	C3−C4	1.370(4)
Ti1−N1	2.105(2)	C4−C5	1.504(4)
Ti1−N2	2.139(2)	C5−C6	1.504(4)
Ti1−N3	2.042(2)	C6−C7	1.456(4)
Ti1−N4	2.295(2)	C7−C8	1.331(5)
Ti1−C16	2.371(2)	C8−C9	1.501(3)
Ti1−C17	2.459(2)	C9−C10	1.590(4)
Ti1−C18	2.465(2)	C9−C41	1.574(3)
Ti1−C19	2.336(2)	C10−C11	1.523(3)
O1−C41	1.422(3)	C11−C12	1.366(6)
N1−C1	1.393(3)	C12−C13	1.412(5)
N1−C4	1.398(3)	C13−C14	1.357(5)
N2−C6	1.299(3)	C14−C15	1.507(3)
N2−C9	1.483(3)	C15−C16	1.515(4)
N3−C11	1.381(3)	C16−C17	1.413(3)
N3−C14	1.396(3)	C17−C18	1.399(3)
N4−C16	1.365(3)	C18−C19	1.405(3)
N4−C19	1.384(3)	C19−C20	1.504(4)
C1−C2	1.361(5)	C41−C42	1.519(3)
C2−C3	1.416(5)		
N3−Ti1−N4	98.2(1)	Ti1−N3−C11	127.9(2)
N2−Ti1−N4	146.3(1)	C11−N3−C14	106.7(2)
N2−Ti1−N3	79.7(1)	Ti1−N4−C19	74.2(1)
N1−Ti1−N4	80.7(1)	Ti1−N4−C16	76.1(1)
N1−Ti1−N3	135.5(1)	C16−N4−C19	106.6(2)
N1−Ti1−N2	78.0(1)	N2−C9−C8	102.8(2)
Ti1−O1−C41	123.5(1)	C8−C9−C41	113.3(2)
Ti1−N1−C4	132.1(2)	C8−C9−C10	111.2(2)
Ti1−N1−C1	120.3(2)	N2−C9−C41	101.5(2)
C1−N1−C4	105.5(2)	N2−C9−C10	110.8(2)
Ti1−N2−C9	109.9(1)	C10−C9−C41	116.0(2)
Ti1−N2−C6	137.2(2)	O1−C41−C9	108.8(2)
C6−N2−C9	109.1(2)	C9−C41−C42	113.8(1)
Ti1−N3−C14	124.5(2)	O1−C41−C42	109.7(2)

hindrance of the novel ligand causes a change in the bonding mode of the porphyrinogen skeleton from η^1-η^1-η^1-η^1 in **1**[8] to η^1-η^1-η^1-η^5 in **3**. The Ti−centroid distance to the D pyrrolic ring, 2.071(2) Å, is quite close to those found in $[(cp)_2Ti]$ derivatives.[17] Titanium shows a distorted square pyramidal coordination with the N_4 set defining the basal plane. The Ti−O1 direction forms a dihedral angle of 30.2(1)° with the normal to the basal plane. The N_4 core shows tetrahedral distortions ranging from −0.081(2) to 0.084(2) Å, with titanium displaced by 0.685(1) Å toward O1. The macrocycle assumes a conformation with the opposite B and D pyrrole rings tilted upward and the opposite A and C rings downward with respect to the N_4 core ("up" means the side of the N_4 plane tilted toward the O1 oxygen), the dihedral angles formed with the N_4 core being 44.7(1), 41.7(1), 19,9(1), and 80.6(1)° for the A, B, C, and D rings, respectively. The Ti−N bond distances associated with uncharged N1 [Ti−N1, 2.105(2) Å] and N2 [Ti−N2, 2.139(2) Å] forming N···H−C hydrogen bonding [N1···C43, 3.583(4) Å; N1···H43, 2.62 Å; N1···H43···C43, 165°] are particularly long compared to those in **1** and Ti−N3 [2.042(2) Å]. The five-membered metallacycle [Ti,O1,C41,C9,N2] has an envelope conformation. The C9 is displaced by 0.645(2) Å from the mean plane through N_4 and is almost perpendicular to it [dihedral angle 97.01(1)°]. The C41−O1, C41−C9, N2−N6, C7−C8, and Ti−O1 distances (Table 2) support the bonding sequence given in Scheme 1.

The α-carbon in the pyrrolyl anion is particularly sensitive to electrophilic attack, as shown by the synthesis of the starting macrocycle,[2] and redox chemistry emphasized by its transformation into artificial porphyrins[3,4] (Scheme 2).

(17) Bochmann, M. In *Comprehensive Organometallic Chemistry II*; Wilkinson, G., Stone, F. G. A., Abel, E. W., Eds.; Pergamon: Oxford, U.K., 1995; Vol. 4; Chapter 5.

Scheme 1

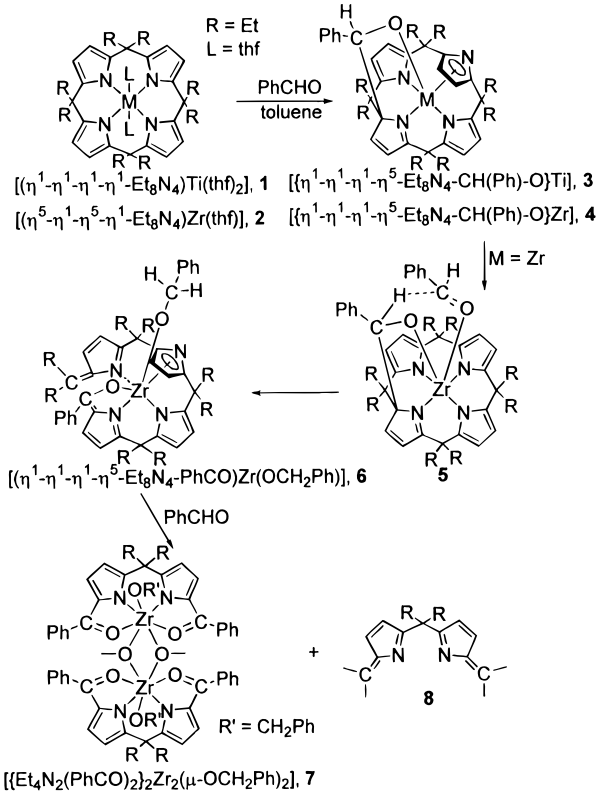

Scheme 2

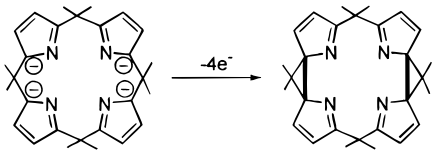

Attempts to demetalate **3** and to free the corresponding pentadentate macrocycle *via* hydrolysis led, instead, to the original *meso*-octaethylporphyrinogen and benzaldehyde reversing the condensation process of **1** to **3**. The same process from **3** to **1** can be reversed by reacting **3** with strong nucleophiles such as LiMe which removes PhCHO from **3** and re-forms **1**.

Due to its higher oxophilicity and coordination number, zirconium drives the reactions in Scheme 1 much further than titanium; thus, **4** might be not isolated. Our investigation focused, however, on the subsequent reaction products. The following step requires 2 equiv of PhCHO and proceeds to **6**, without any possibility of intercepting intermediates like **4** and **5**.

The coordination of a second molecule of PhCHO on zirconium, which achieves the coordination number 7, results in the juxtapositioning of an alcoholic and a carbonylic function. As in the case of Al^{3+}, zirconium assists the so-called Meerwein−Ponndorf reduction,[18] with the hydrogen transfer from the alcoholic to the carbonylic function *via* a cyclic transition state similar to that shown schematically for **5**. This causes the cleavage of the C−C between the pyrrole and the *meso*-carbon and affords the structure shown for **6** (see also Figure 2).

Complex **6** has been isolated as yellow-orange crystals. Its structure allows us to understand the further transformation in the reaction with benzaldehyde.

(18) March, J. *Advanced Organic Chemistry*, 3rd ed.; Wiley: New York, 1985; p 913.

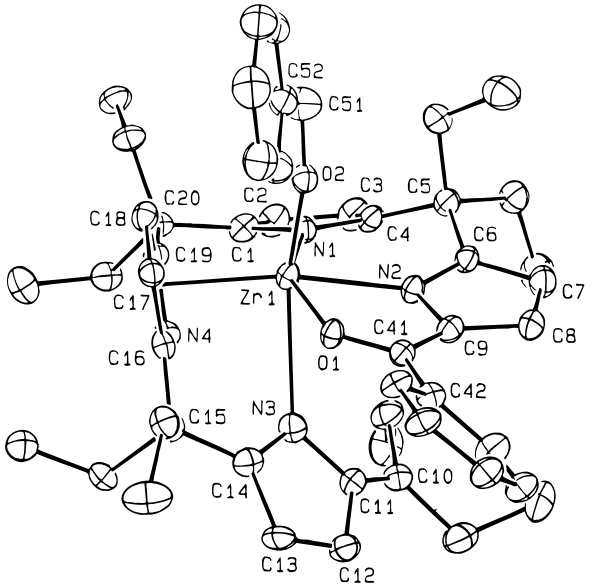

Figure 2. ORTEP view of the structure of complex **6** (50% probability ellipsoids).

Table 3. Selected Interatomic Distances (Å) and Angles (deg) for Complex **6**

Zr1−O1	2.236(4)	C2−C3	1.411(8)
Zr1−O2	1.923(4)	C3−C4	1.374(7)
Zr1−N1	2.192(3)	C4−C5	1.530(7)
Zr1−N2	2.222(3)	C5−C6	1.508(7)
Zr1−N3	2.616(3)	C6−C7	1.430(7)
Zr1−N4	2.445(3)	C7−C8	1.373(8)
Zr1−C16	2.491(5)	C8−C9	1.404(7)
Zr1−C17	2.598(5)	C9−C41	1.407(7)
Zr1−C18	2.628(4)	C10−C11	1.356(7)
Zr1−C19	2.509(4)	C11−C12	1.441(7)
O1−C41	1.282(6)	C12−C13	1.351(7)
O2−C51	1.384(6)	C13−C14	1.451(7)
N1−C1	1.408(5)	C14−C15	1.504(7)
N1−C4	1.402(6)	C15−C16	1.514(7)
N2−C6	1.328(6)	C16−C17	1.405(7)
N2−C9	1.391(6)	C17−C18	1.402(7)
N3−C11	1.427(6)	C18−C19	1.409(5)
N3−C14	1.321(6)	C19−C20	1.516(6)
N4−C16	1.386(6)	C41−C42	1.477(6)
N4−C19	1.366(5)	C51−C52	1.506(8)
C1−C2	1.374(7)	C52−C53	1.392(8)
N3−Zr1−N4	65.0(1)	Zr1−N3−C11	133.1(3)
N2−Zr1−N4	139.8(1)	C11−N3−C14	106.5(4)
N2−Zr1−N3	82.2(1)	Zr1−N4−C19	76.6(2)
N1−Zr1−N4	86.3(1)	Zr1−N4−C16	75.5(2)
N1−Zr1−N3	104.6(1)	C16−N4−C19	106.9(3)
N1−Zr1−N2	79.9(1)	N2−C9−C8	108.9(4)
O1−Zr1−O2	85.7(1)	C8−C9−C41	135.3(4)
Zr1−O1−C41	118.0(3)	N2−C9−C41	115.0(3)
Zr1−O2−C51	167.1(3)	C25−C10−C27	116.3(4)
Zr1−N1−C4	130.5(3)	C11−C10−C27	122.2(5)
Zr1−N1−C1	121.7(3)	C11−C10−C25	121.4(5)
C1−N1−C4	105.5(4)	O1−C41−C9	118.5(4)
Zr1−N2−C9	116.2(3)	C9−C41−C42	123.2(4)
Zr1−N2−C6	135.1(3)	O1−C41−C42	118.2(4)
C6−N2−C9	108.0(3)	O2−C51−C52	114.7(4)
Zr1−N3−C14	110.6(3)		

The coordination polyhedron around zirconium is a distorted tetragonal bipyramid, with the apical sites occupied by the O2 and N3 atoms and the best equatorial plane defined by O1, N1, N2 and the centroid of the η^5-bonded D pyrrole ring [Zr−Cp4, 2.240(4) Å]. The metal is displaced by 0.166(1) Å from the equatorial plane which shows significant tetrahedral distortions ranging from −0.050(4) to 0.062 Å. The Zr−O2 bond distance [1.923(4) Å] is significantly shorter than the Zr−O1 bond distance [2.236(4) Å] in agreement with the values of the O−C bond distances and Zr−O−C bond angles indicating a single bond character of the O2−C51 bond [1.384(6) Å] and a partial double bond character of the O1−C41 bond [1.282(6) Å].

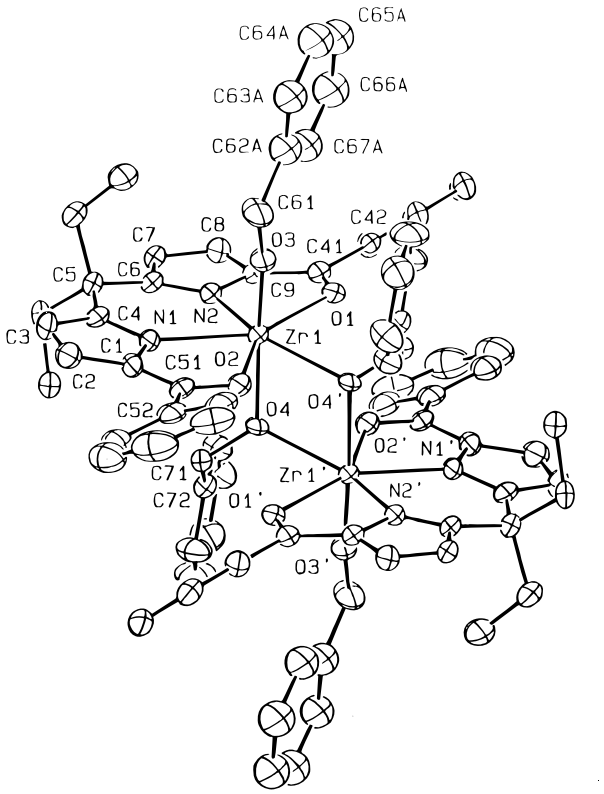

Figure 3. ORTEP view of the structure of complex **7** (50% probability ellipsoids). Prime denotes a transformation of $1 - x, -y, 1 - z$. The B position of the disordered C62−C67 aromatic ring has been omitted for clarity.

Scheme 3

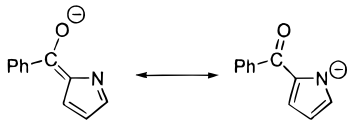

As far as the latter point is concerned, the structural parameters (Table 3) related to the benzoyl group α-bonded to the pyrrole B allow us to write down equally well the two bonding sequences shown in Scheme 3.

Accordingly, this system is nearly planar, the displacements from the planarity ranging from −0.119(5) to 0.100(5) Å. The dihedral angle between the pyrrole and the metallacycle is 9.7-(2)°. The cleavage of C−C at the *meso*-position occurs with the formation of the C10−C11 [1.356(7) Å] double bond and as a consequence the bonding sequence shown for the C pyrrole, which interacts very weakly with zirconium at a distance of 2.616(3) Å. The weakly bonded nitrogen, N3, can be easily displaced by an incoming molecule of PhCHO which, through the same pathway, cleaves a second *meso*-bridge and leads to the formation of **7** and to the extrusion of **8**. Complex **7** can be obtained either by reacting **2** with 4 equiv, eventually an excess of PhCHO, or by reacting **6** with 2 equiv of PhCHO under the same conditions. The rearrangement of the monomeric precursor to a dimeric form like **7** (see Figure 3) is not chemically relevant. The reaction ends up with the formation of a quadridentate dianionic N_2O_2 chelating ligand which is the deprotonated form of the dibenzoyl-α,α′-dipyrromethane. The synthesis of diacyl-α,α′-dipyrromethanes can be performed

Table 4. Selected Bond Distances (Å) and Angles (deg) for Complex **7**[a]

Zr1−O1	2.223(4)	C1−C2	1.409(7)
Zr1−O2	2.236(4)	C1−C51	1.402(8)
Zr1−O3	1.906(4)	C2−C3	1.357(11)
Zr1−O4	2.201(4)	C3−C4	1.415(9)
Zr1−O4′	2.159(4)	C4−C5	1.506(10)
Zr1−N1	2.296(5)	C5−C6	1.516(9)
Zr1−N2	2.292(5)	C6−C7	1.407(10)
O1−C41	1.274(8)	C7−C8	1.376(8)
O2−C51	1.278(7)	C8−C9	1.417(9)
O3−C61	1.411(9)	C9−C41	1.403(7)
O4−C71	1.425(6)	C41−C42	1.491(8)
N1−C1	1.405(9)	C51−C52	1.480(10)
N1−C4	1.343(7)	C61−C62A	1.654(10)
N2−C6	1.334(7)	C61−C62B	1.406(9)
N2−C9	1.405(8)	C71−C72	1.508(8)
N1−Zr1−N2	73.5(2)	Zr1−N2−C6	138.7(4)
O3−Zr1−O4′	171.1(2)	C6−N2−C9	106.3(5)
O2−Zr1−N1	70.8(2)	N1−C1−C51	115.8(5)
O2−Zr1−O4	74.5(1)	N1−C1−C2	109.0(5)
O1−Zr1−N2	70.3(2)	C2−C1−C51	134.8(6)
O1−Zr1−O4	73.7(2)	N2−C9−C8	109.4(4)
O1−Zr1−O2	145.6(1)	C8−C9−C41	135.2(5)
Zr1−O1−C41	121.0(3)	N2−C9−C41	114.8(5)
Zr1−O2−C51	119.9(3)	O1−C41−C9	118.1(5)
Zr1−O3−C61	166.9(4)	C9−C41−C42	122.9(5)
Zr1−O4−Zr1′	107.6(2)	O1−C41−C42	118.7(5)
Zr1′−O4−C71	126.3(3)	O2−C51−C1	118.5(5)
Zr1−O4−C71	122.0(3)	C1−C51−C52	122.7(5)
Zr1−O4′−Zr1′	107.6(2)	O2−C51−C52	118.7(5)
Zr1−N1−C4	138.2(4)	O3−C61−C62B	125.0(6)
Zr1−N1−C1	114.3(4)	O3−C61−C62A	103.7(5)
C1−N1−C4	106.3(5)	O4−C71−C72	113.8(4)
Zr1−N2−C9	114.9(3)		

[a] Prime denotes a transformation of $1 - x, -y, 1 - z$.

either from the direct acylation of the dipyrromethane[19] or from the reaction reported here, using **2** as starting material. The latter method can be a quite convenient synthesis, due to the availability of the *meso*-octaalkylporphyrinogen complexes. In addition, it leads directly to the corresponding metalated form. The structural parameters (Table 4) support the bonding scheme given in the picture for each monomeric unit of **7**, with a charge delocalization, as shown in Scheme 3, between nitrogen and oxygen for each half of the quadridentate ligand.

The two N···O systems are nearly planar [displacements ranging from −0.059(5) to 0.052(6) and from −0.075(5) to 0.046(5) Å for N1···O2 and N2···O1, respectively], and the dihedral angle they form is 11.4(1)°. The two monomeric units are bonded in centrosymmetric dimers by the bridging alkoxo oxygens O3 and O4. The coordination polyhedron around zirconium could be described as a distorted pentagonal bipyramid with the equatorial plane defined by the nitrogen and oxygen atoms of the N_2O_2 core and by the O4 oxygen atom [displacements in the range ±0.299(4) Å]. The axial positions are occupied by the O3 and O4′ oxygen atoms ($' = 1 - x, -y, 1 - z$), the Zr−O3 and Zr−O4′ lines forming dihedral angles of 2.9(1) and 7.9(1)°, respectively, with the normal to the equatorial plane. Zirconium is displaced from it by 0.114(1) Å toward O3. The Zr,N1,C1,C51,O2 and Zr,N2,C9,C41,O1 five-membered chelate rings are nearly planar [displacements ranging from −0.058(5) to 0.043(5) and from −0.066(5) to 0.074(5) Å, respectively] and coplanar with the adjacent A and B pyrrole rings, the dihedral angles they form being 8.5(2) and 7.1(1)°, respectively. The Zr,N1,C4,C5,C6,N2 six-membered chelate ring assumes a flattened half-boat conformation, the C5 *meso*-carbon atom being displaced by 0.200(5) Å from the mean plane through the other atoms. As a possible consequence of the seven-coordinate metal, the Zr−N bond distances [mean value 2.294(5) Å] are significantly longer than the corresponding Zr−N2 bond distance in complex **6**. The Zr−O1 [2.223(4) Å] and Zr−O2 [2.236(4) Å] bond distances involving the oxygen atoms of the benzoyl groups as well as the Zr−O3 bond distance [1.906(4) Å] involving the oxygen atoms of the alkoxo ligands agree well with the corresponding values observed in **6**. The Zr−O4 bond distance [2.201(4) Å] is remarkly longer than Zr−O3 as expected by the bridging role of the O4 oxygen atom.

The metal-assisted electrophilic activation of the porphyrinogen skeleton sheds light on some of the important processes in which porphyrinogen is involved, such as the macrocyclic ring closure and opening and its degradation to dipyrromethane moieties. From a synthetic point of view, such reactions can be adapted to major synthetic purposes: (*i*) the functionalization of the porphyrinogen skeleton; (*ii*) the synthesis of novel polydentate ligands derived from α,α′-dipyrromethane.

Acknowledgment. We thank the "Fonds National Suisse de la Recherche Scientifique" (Grant No. 20-40268.94) and Ciba-Geigy SA (Basel, Switzerland) for financial support.

Supporting Information Available: Tables of experimental details associated with data collections and structure refinements, final atomic coordinates for non-H atoms, hydrogen atom coordinates, thermal parameters, and bond distances and angles for **3**, **6**, and **7** (17 pages). Ordering information is given on any current masthead page.

IC961446C

(19) Lee, C.-H.; Li, F.; Iwamoto, K.; Dadok, J.; Bothner-By, A. A.; Lindsey, J. S. *Tetrahedron* **1995**, *51*, 11645−11672.